PARD BIENNIAL INSPECTION 1951

Introduction and Pulse Model

Presented by W. M. Bland, Jr., A. J. Vitale, E. M. Fields,
and C. T. D'Aiutolo

You are now in the model assembly shop of the Pilotless Aircraft Research Division. Extensive use of rocket-propelled free-flight models launched from the ground has enabled this division of the Langley Laboratory to gather quickly large amounts of varied information about aerodynamic behavior in the transonic and supersonic speed ranges. For some time these rocket-model techniques have been a principal source of large-scale transonic and supersonic information. During your visit here today some of the techniques for obtaining aerodynamic data from rocket models will be discussed and you will be given an opportunity to view some of the test models and equipment.

Rocket-model techniques for obtaining aerodynamic data at transonic and supersonic speeds involve rockets, radar, telemetering, and motion-picture camera tracking combined with a suitable test vehicle and measuring instruments. The rocket motors, which are of the solid propellant type, are used as a means of propulsion to accelerate the test vehicle to the desired speed. Radar is used to determine the location of the model in space and its velocity at any time during the flight. A special type of radio system known as telemetering is used to obtain a recording of the various aerodynamic reactions of the models as measured by instruments installed in the models. Motion-picture cameras are used to obtain a visual record of the initial phase of the flight. The models are instrumented here at the Langley Laboratory, but the actual flight tests are conducted at Wallops Island, a sparsely settled area located on the Atlantic Ocean near the Maryland-Virginia state line. This is an aerial photograph of the test station, where the models

are launched from this area out to sea. Here is a photograph of one of the models immediately after takeoff.

There are many combinations of models, instruments, rockets, radar, and telemetering. These combinations are used to investigate many aerodynamic problems, some of which are listed here, (chart) lift and drag, control effectiveness, damping in roll, inlet performance, flutter, buffeting, boundary-layer phenomena, and the complete longitudinal and lateral flying qualities of airplane and missile configurations. In all of these investigations the data are obtained continuously from high subsonic speeds, through the transonic region, and as far into the supersonic region as desired.

Here is a general research vehicle used to investigate the longitudinal flying qualities of various airplane configurations. The hatches have been removed so that you can see some of the equipment. This is the telemetering unit capable of detecting and transmitting ten separate items of information continuously to ground receiving and recording stations. The complete weight of this unit including the batteries is about 13 pounds and it is so rugged that it can withstand loads which are greater than 100 "g's". Here can be seen an angle of attack indicator, which measures the direction of the air relative to the model. These are the pressure pickups used to obtain Mach number, and here are the so-called accelerometers which are used to measure the total aerodynamic forces acting on the model. The wing is mounted on a beam-type balance which measures wing lift. The antenna for transmitting the telemeter signals to ground receiving and recording stations is located along the leading edge of the vertical tail. The horizontal tail is moved in an approximately square wave periodic motion during flight by a hydraulic

power system located here. The model is propelled to supersonic speeds by a booster rocket, that is, by a rocket motor which, after expending its fuel, separates from the model, allowing the model to fly freely through the air.

After the model is free from the booster it responds to the movement of the horizontal tail in a manner such that aerodynamic data are obtained throughout the angle of attack range. The motion of an airplane after a sudden control deflection will be demonstrated by this flight simulator. The time history of the control deflection, angle of attack, and lift will be shown here.

Control moves - model oscillates with decreasing amplitude - trims at new angle of attack - etc. (About 2 up and 2 down control movements.)

From the flight of one pulsed control model such as this, the following aerodynamic data are obtained continuously from high subsonic speeds through the transonic range and far into the supersonic region. (Chart) Lift, both total and wing lift; drag, minimum and induced; static longitudinal stability; dynamic longitudinal stability; trim; control effectiveness; and hinge moments.

Mr. will now discuss another rocket-model technique.

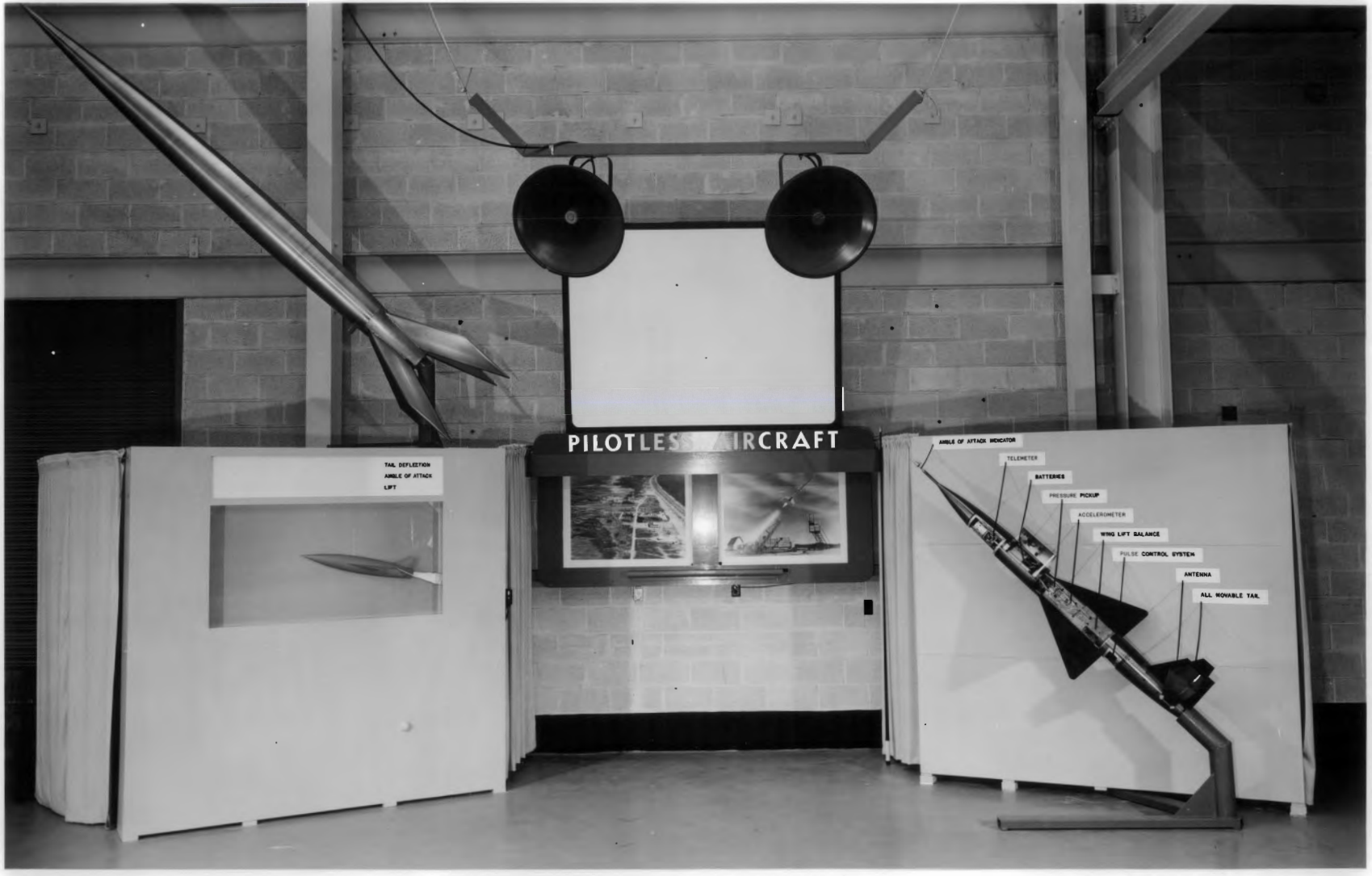

NACA

LAL 70501

NACA

LAL 70500

PILOTLESS AIRCRAFT

ROCKET MODELS
TYPES OF INVESTIGATIONS

- LIFT AND DRAG
- CONTROL EFFECTIVENESS
- HINGE MOMENTS
- DAMPING IN ROLL
- INLET PERFORMANCE
- FLUTTER
- BOUNDARY LAYER PHENOMENA
- AUTOMATIC STABILIZATION
- STABILITY AND FLYING QUALITIES OF AIRPLANES AND MISSILES

PULSED ELEVATOR MODELS
DATA OBTAINED

TOTAL LIFT	$C_{L_\alpha}, C_{L_{max}}$
WING LIFT	$C_{L_{\alpha_w}}$
DRAG	$C_{D_{min}}, dC_D/dC_L{}^2$
STATIC STABILITY	$C_{m_\alpha}, C_{m_{C_L}}$, a.c.
DYNAMIC STABILITY	$C_{m_{\dot\theta}} + C_{m_{\dot\alpha}}$
TRIM	$C_{L_{TRIM}}, \alpha_{TRIM}$
CONTROL EFFECTIVENESS	$C_{m_\delta}, C_{L_\delta}$
	$(\alpha/\delta)_{TRIM}, (C_L/\delta)_{TRIM}$
HINGE MOMENTS	$C_{h_\delta}, C_{h_\alpha}$

NACA

LAL 70503

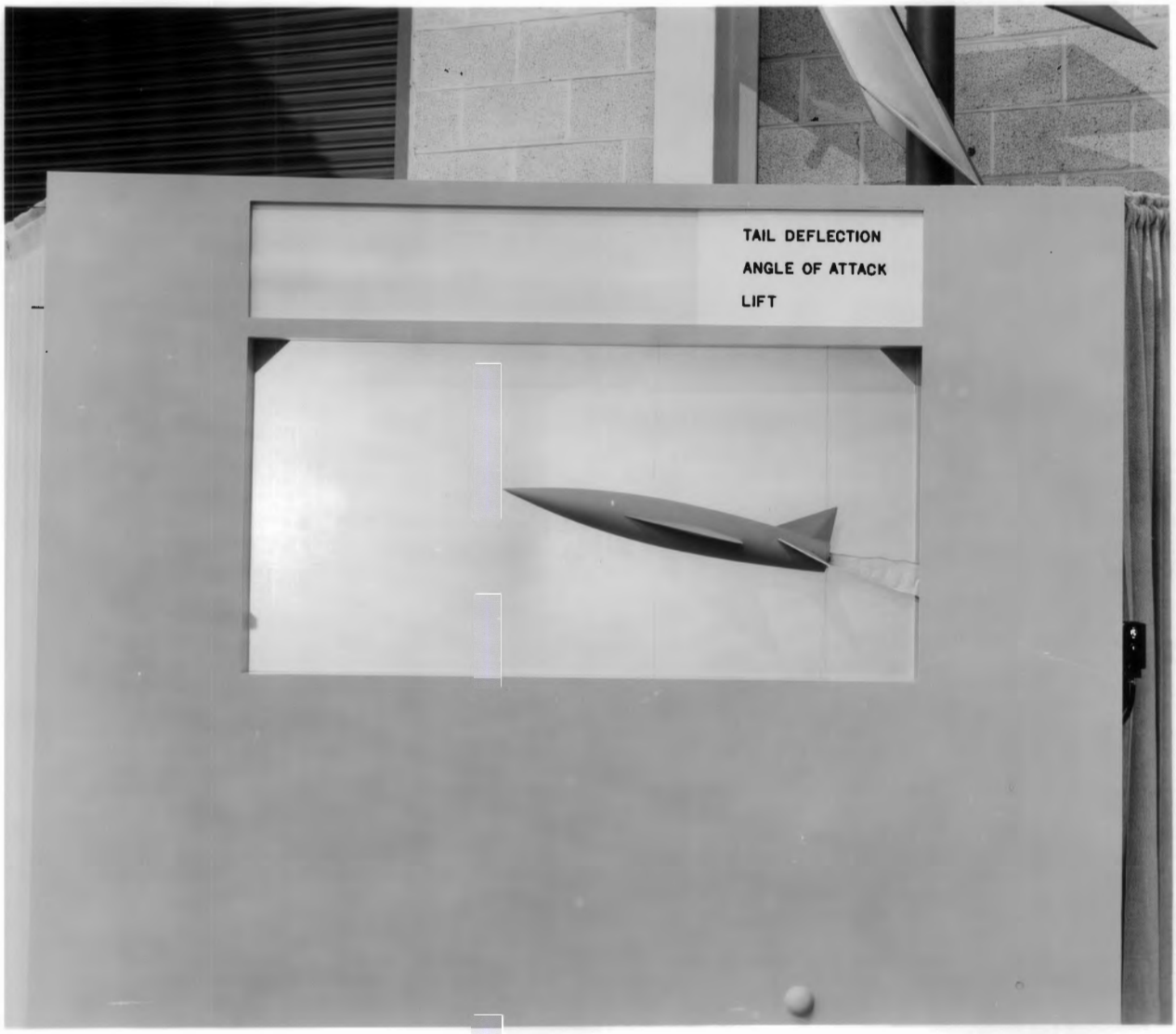

NACA

LAL 70510

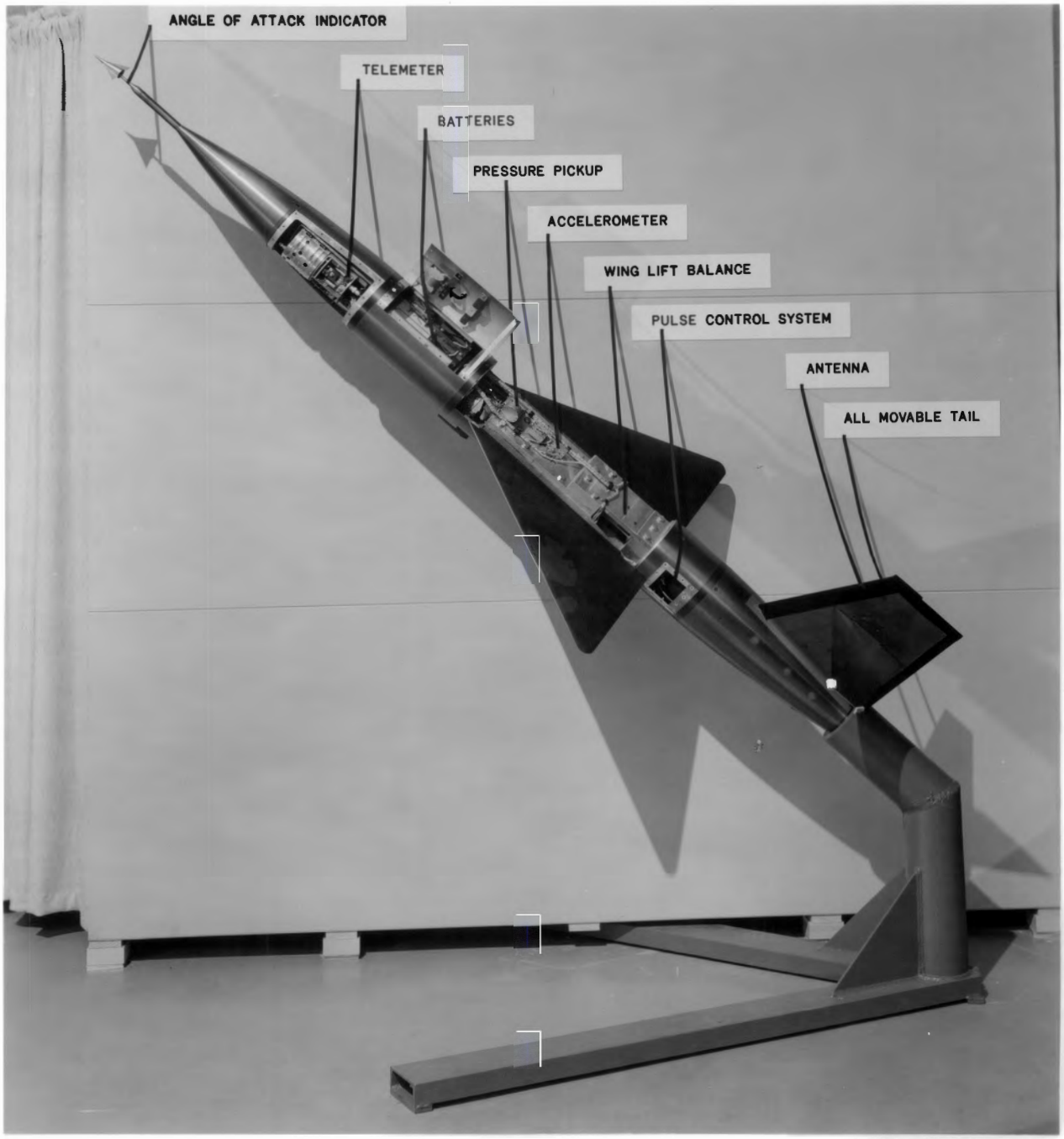

NACA

LAL 70511

Boundary-Layer Survey and Movie

Presented by J. D. Church, A. H. Hinners, A. E. Dietz,
and T. L. Kennedy

This model is used to investigate boundary-layer and skin-friction phenomenon at supersonic speeds. The distribution of total pressure through the boundary layer is measured with this six-tube total-pressure rake located on the aft portion of this parabolic body. The local static pressure is measured with a flush orifice in the skin. Here is a chart illustrating the characteristics of a boundary layer at a free-stream Mach number of approximately 3.

The total pressure distribution varies from the free-stream total pressure value to the local static pressure at the skin surface.

Here is the velocity distribution which is obtained from these pressures and from measured and calculated temperatures. At the skin surface, the velocity has a zero value, yet at only 1/16 of an inch from this surface, the velocity is approximately 2/3 of the free-stream value and varies smoothly through the boundary layer to the free-stream value. Hence, the importance of a smooth, polished skin is evident.

The loss of momentum in the boundary layer, which is a measure of the skin-friction drag, is then obtained by integration of the velocity-density relation through the boundary layer.

Before discussing other rocket-model techniques we will show you by means of a motion picture some views of the Wallops Island test station and equipment and some actual model flights.

Movie

This is an aerial view of the Wallops Island test station. Here is the launching area from which the models are fired out to sea. This is the final assembly shop where the test vehicles are prepared for launching. Here is the building which houses the electronic receiving and recording instrumentation. This is the control tower from which all the model launchings are coordinated.

Here is a close-up view of the preflight testing facility where ramjet engines and inlet investigation models are placed in an air jet for calibration and final adjustment prior to actual testing on rocket-propelled vehicles. The spheres shown here are the air storage tanks for this facility.

This is a ramjet engine mounted in position for a ground test in a Mach number 2 air jet. The fuel control system and starting mechanism are being checked before the engine is flown on a free-flight test vehicle. The glowing of the combustion chamber indicates the large amount of energy being released. These "Mach diamonds" in the exhaust show that it is supersonic.

This is an inlet investigation model and its booster rocket on the launcher. Here can be seen the takeoff of this model.

This is another view of the model takeoff and flight. Note the booster rocket being rejected from the model, leaving the vehicle to fly freely at supersonic speeds.

This radar is tracking the model to determine its velocity. Another radar unit shown here is recording the position of the model in space throughout the entire flight. (Statements about radiosonde must be made while the

584 is still on the picture). Immediately after the test, a radiosonde balloon is released to determine the pressure, temperature, and density of the air through which the model has flown.

The model on the launcher is a research vehicle used to investigate the large-scale drag characteristics of airplane configurations. This model has a rocket motor within the fuselage. There is takeoff. This is another view of the takeoff and flight of the model. Note that, in this case, after expenditure of fuel the model flies freely without the need of separation from a booster. The maximum Mach number of this flight was about 1.5.

The next scene is the launching of a nacelle drag research model. This illustrates the two-stage rocket technique. The model takes off under the power of a booster rocket, and after the expenditure of its fuel is rejected from the model. A sustainer rocket in the model then propels the model to its maximum speed.

This is the launching of a test vehicle for investigating boundary layer and aerodynamic heating over a wide range of Mach number and Reynolds number. This model also has a two-stage rocket motor. The sustainer firing is delayed so that the model will reach a maximum altitude of some 100,000 feet and a maximum Mach number of approximately 4.0.

It should be pointed out at this time that all of the model launching pictures are shown in slow motion. The actual flight motion is approximately 4 times faster than that seen here.

The model shown here is one of the pulsed control vehicles previously discussed. This, again, illustrates the single-stage type of launching. At separation, it can be seen that the model responds to the motion of the pulsed tail.

The final research vehicle shown is used to investigate aerodynamic and automatic stabilization problems associated with missile configurations. Again, a single-stage of propulsion is employed; however, in this case, two rocket motors in parallel are used.

If you will please step over to the area to my right Mr. will discuss other rocket model investigations.

NACA

LAL 70502

1951 BI
PARD
Loposer

Flutter Discussion and Inlet Display

Presented by J. D. Loposer, C. F. Merlet, W. A. Bartlett, Jr., and W. E. Stoney

This is a model used to investigate flutter in the transonic speed range. Test wings of predetermined strength and flexibility are bolted to the wing root casting. The remaining space is filled with a resin plastic to give a rigid root attachment. Strain gages are placed near the wing root to give an indication of wing twisting and bending motions in flight. The model is also instrumented with an angle-of-attack indicator and accelerometers to measure the body motions and to determine if any coupling exists between wing and body modes. A two-stage rocket motor carries the model through the test Mach number range at a forward acceleration of about 8 g's.

Here is an actual telemeter record of the flight of one of these models. These two oscillating channels marked wing bending and wing torsion indicate the motions of the wings as sensed by the strain gages. When flutter begins, the amplitude of the wing motions builds up very rapidly so that the wing is destroyed after 10 or 20 cycles or at about this point. However, in this test the wings fluttered at a Mach number slightly greater than 1 and did not fail even at the maximum Mach number of the test (slightly greater than 1.5). The greatest amplitude of flutter occurred at about 1.2 Mach number.

Tests such as these enable us to modify and extend existing flutter theory for use in the design of modern high-speed aircraft.

Inlet Display

A method has been developed to obtain air inlet performance throughout the Mach number range and over a wide range of air flows. Here is a typical

model with a scoop type inlet. The air enters the model here, and is led through a diffuser to an air flow regulator located here. The regulator is continuously operated in flight by this electric motor.

This is a cutaway view showing the internal portion of the air flow regulator with the shutters rotating. The rotation of the shutters causes the air flowing through this mockup to increase and decrease periodically, as shown by the rise and fall of the tufts.

This is a time history of the data obtained during the supersonic portion of the flight of one of these models. The lower curve shows how the air flow varies. The middle curve shows the total pressure recovery, which is a measure of duct efficiency. The upper curve presents the model external drag. Note the periodic change in both pressure recovery and drag with varying air flow. The maximum values of pressure recovery and drag occur when the air flow is at a minimum.

Thus, data on inlet performance are obtained for the many different conditions that may be required by modern jet engines.

NACA

LAL 70506

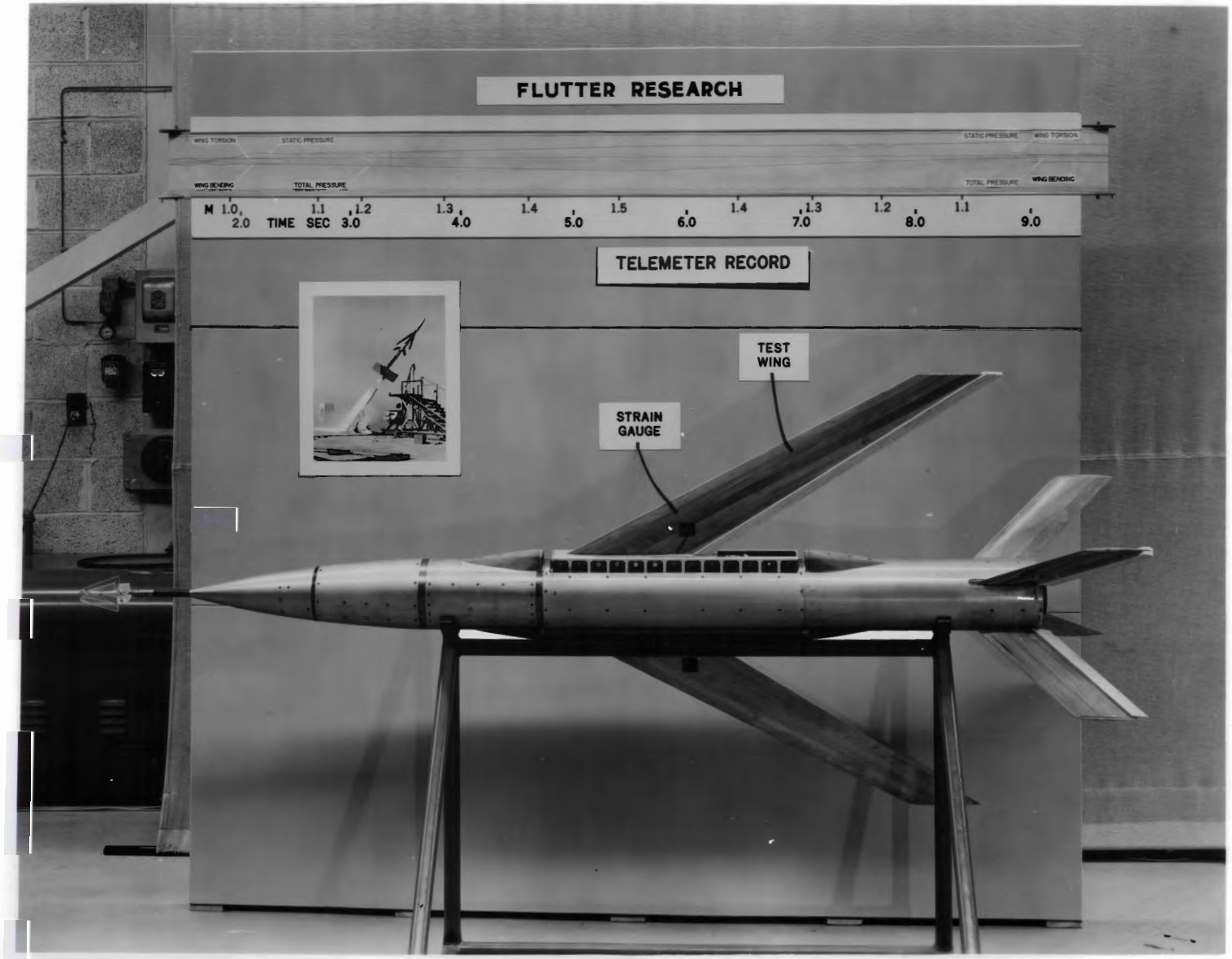

NACA

LAL 70504

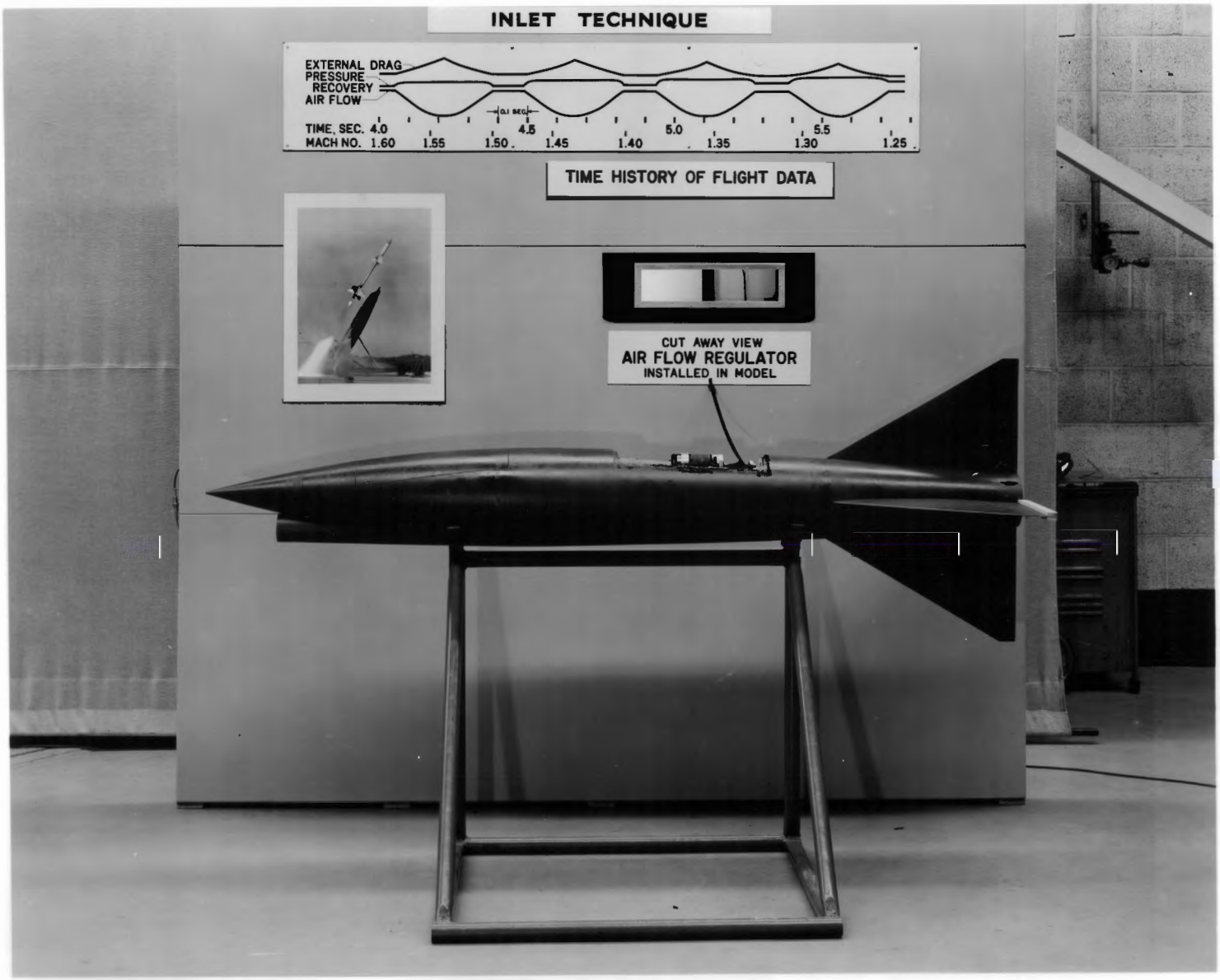

NACA

LAL 70505

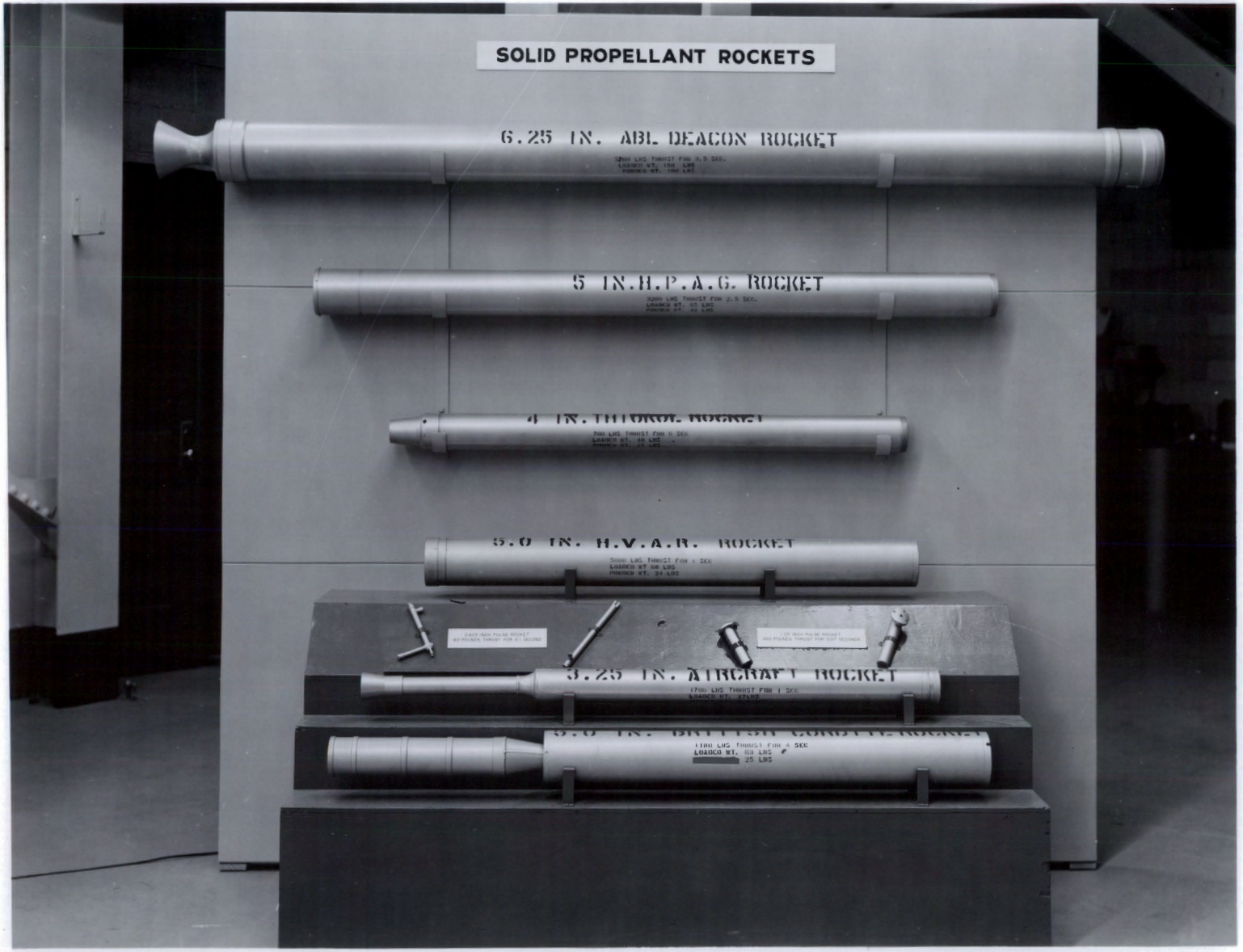

NACA

LAL 70507

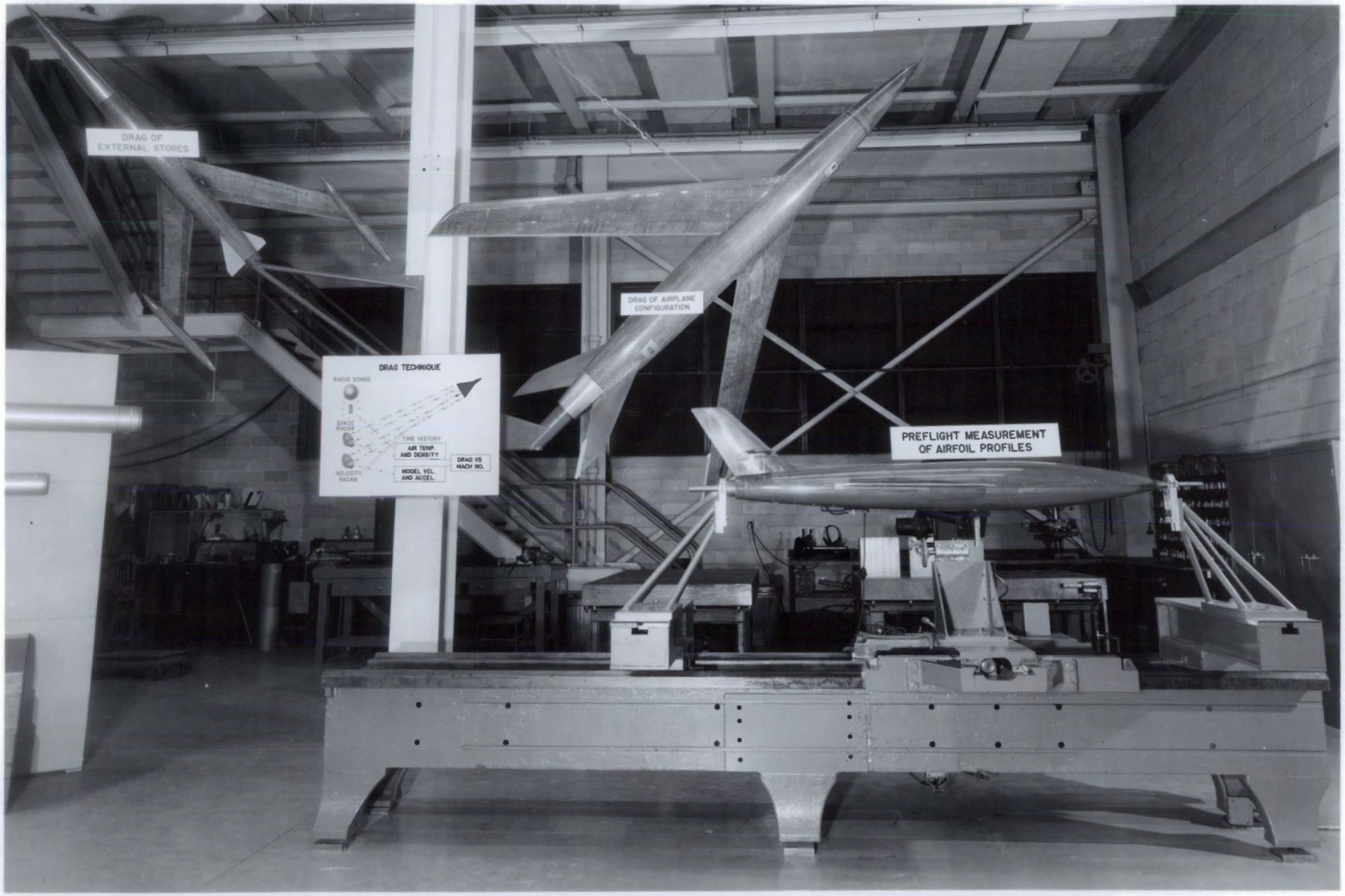

NACA

LAT. 70508

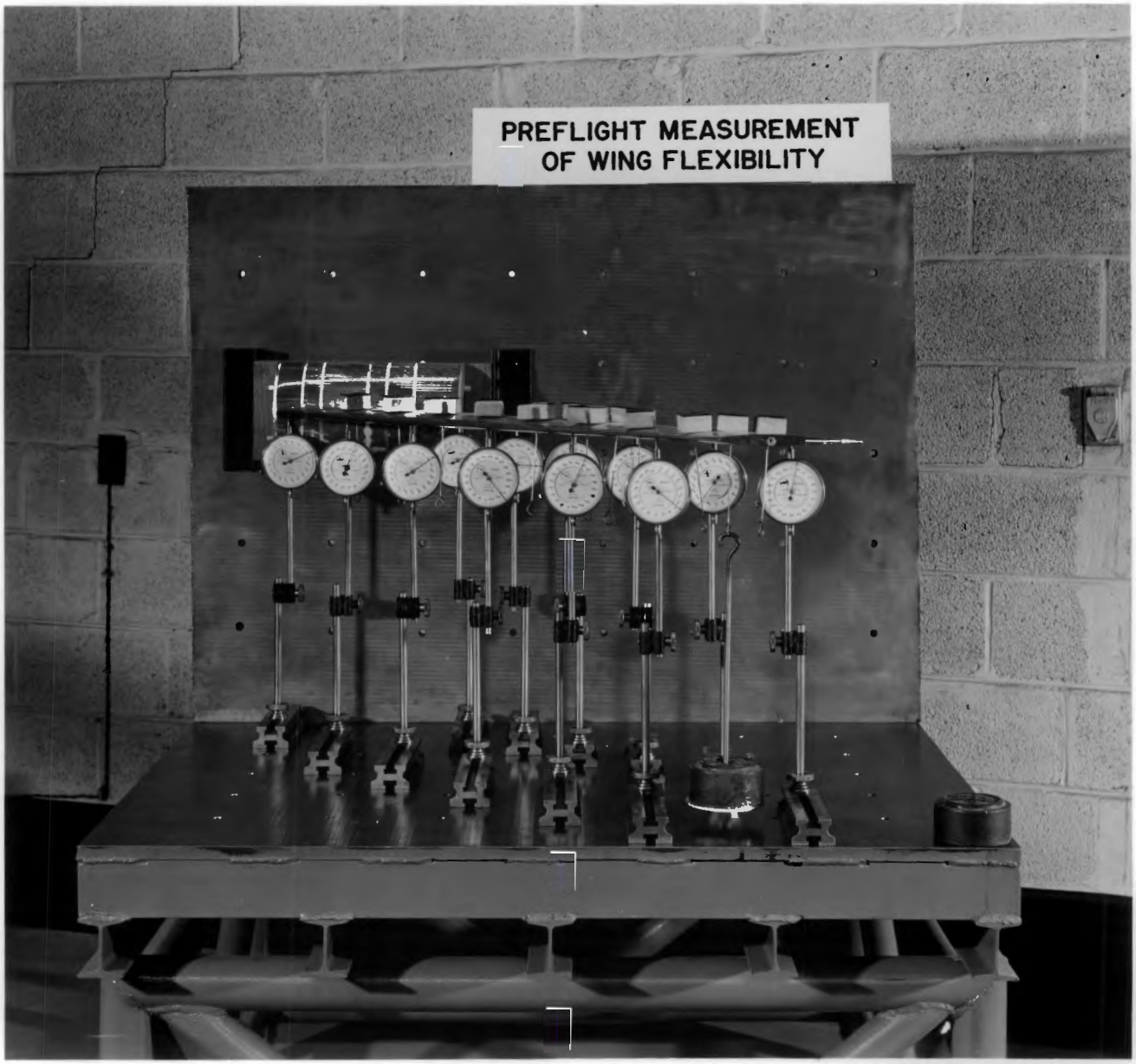

NACA

LAL 70509

NACA

LAL 70475

INLETS AND CASCADES

INLET DRAG AT TRANSONIC SPEEDS

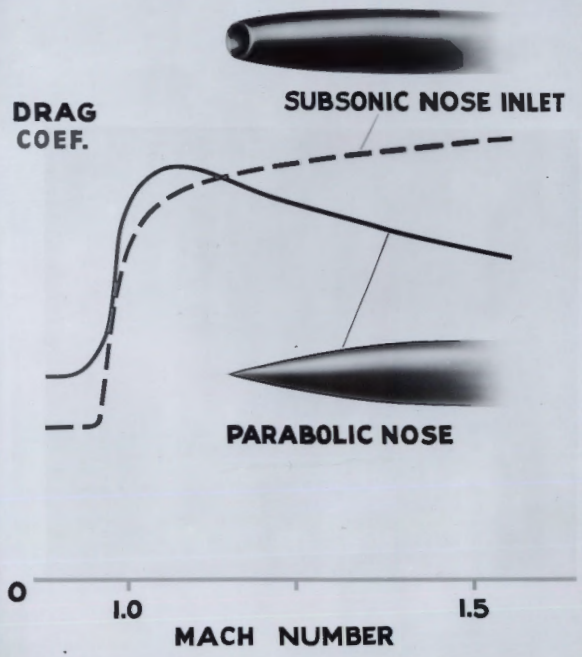

INLET AREA PROBLEM FOR SUPERSONIC INLETS

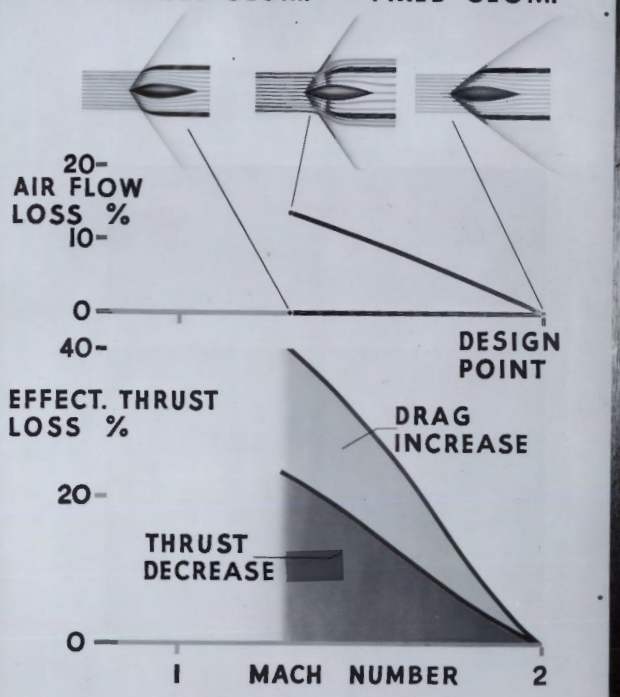

NACA

LAI. 70477

INLETS AND CASCADES

SUPERSONIC SIDE INLET DERIVED FROM NOSE INLET

NOSE INLET

SIDE INLET WITH NO B.L. BYPASS

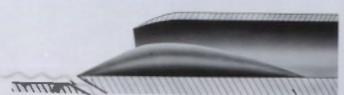

SIDE INLET WITH B.L. BYPASS

RAM PRESSURE AT ENGINE

NACA

LAL 70478